

Longitudinal analysis of Disturbed dynamo magnetic signatures

Castellanos-Velazco C. I.^{1,3}

Corona-Romero P.^{2,3}

Sergeeva M.^{2,3}

¹Universidad Nacional Autonoma de Mexico, Posgrado en Ciencias de la Tierra

² Laboratorio Nacional de Clima Espacial

³ Instituto de Geofisica

Abstract

The present study seeks to analyze longitudinally, the magnetic fluctuations associated with the disturbed dynamo electric field (DDEF) using 11 observatories encircling the globe at mid-low latitudes. The event to be studied is the geomagnetic storm known as the Saint Patrick event due to his main phase was developing during that celebration (march 17th, 2015). In the present studio, we perform a wavelet spectrum in combination with cross-wavelet technique and a semblance analysis studio in order to isolate the DDEF magnetic signatures.

Keywords: Disturbed dynamo, wavelet

Contents

1	Introduction	1
1.1	Geomagnetic Data	1
2	Methodology	2
2.1	Processing magnetic data	2
2.2	Isolation of magnetic fluctuations of ionospheric origin	2
2.3	Time-Frequency Analysis	3
3	Results	4
3.1	Fourier Analysis	4
3.2	Wavelet Analysis	4
4	Discussion	4
5	conclusions	4

1 Introduction

During geomagnetic storms (GS), one of the responses which arise in the ionosphere is the driving of electric currents. In the case of mid-low geomagnetic latitude ranges, we highlight the presence of the Disturbed dynamo (Ddyn) and the disturbed polar current number 2 (DP2).

1.1 Geomagnetic Data

The geomagnetic data analyzed in this paper corresponded to the observatories shown within the Table 1. magnetic data can be obtained from INTERMAGNET (*International Real-Time Magnetic Observatory Network* [5]) where as it is shown, all the observatories are present within the a narrow range of magnetic latitude ($21 - 33^\circ$). On the other hand, this observatories envelope quite different Universal Time (UT) zones. We have to deal with limitations for the aim of this project due to the lack of data availability for some observatories during the period of interest combined with the absence of observatories at some points. In the end it was decided to divide the longitudinal study in five sectors in function of the UT zones for each observatory:

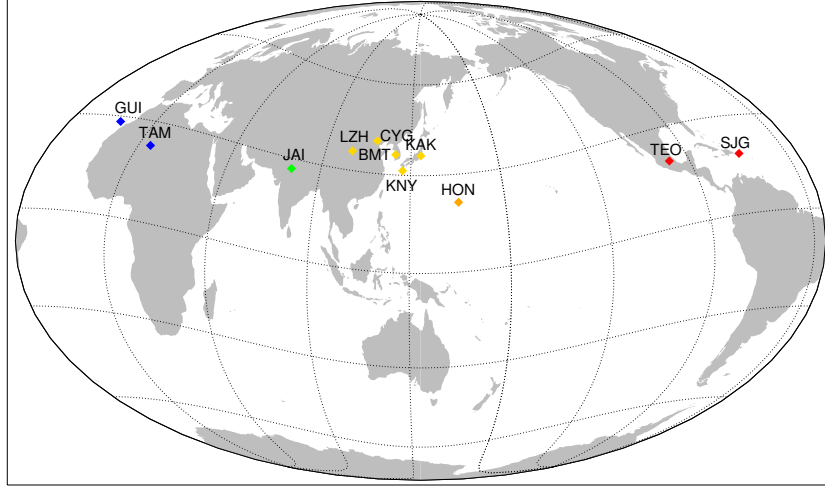


Figure 1: Geographic position of every magnetic observatory considered for this study. The color code corresponds to different local time regions: blue (UT 0, 1), green (UT 5:30), yellow (UT 8, 9), orange (UT -10), red (-6, -4).

1. sector 1: GUI (UTC 0), TAM (UTC 1)
2. sector 2: JAI (UTC 5:30)
3. sector 3: LZH, BMT (UTC 8), CYG, KNY, KAK (UTC 9)
4. sector 4: HON (UTC -10)
5. sector 5: TEO (UTC -6), SJG (UTC -4)

Although the distance between each observatory presents a limitation for studying the longitudinal develop of the GS, we can still analyze the response for different time sectors in which each observatory was present during the main phase.

Table 1: List of observatories considered for this study.

Country	Observatory	IAGA code	geographic latitude	geographyc longitude	magnetic latitude	magnetic longitude	UT h
China	Beijing	BMT	40.3 N	116.2 E	30.53 N	172 W	8
South Korea	Cheongyang	CYG	36.37 N	126.854 E	27 N	162.43 W	9
India	Jaipur	JAI	26.917 N	75.8 E	18.42 N	150.47 E	5.5
Spain	Guimar	GUI	28.317 N	16.433 W	33.21 N	61.1 E	0
USA	Honolulu	HON	21.317 N	158 W	21.49 N	90.03 W	-10
Japan	Kakioka	KAK	36.232 N	140.186 E	27.8 N	149.73 W	8
Japan	Kanoya	KNY	31.417 N	130.867 W	22.3 N	158.4 W	9
China	Lanzhou	LZH	36.083 N	103.833 E	26.23 N	176.79 E	8
USA, Puerto Rico	San Juan	SJG	18.11 N	66.15 W	28.19 N	6.1 E	-4
Argelia	Tamanraset	TAM	22.783 N	5.571 E	24.3 N	82.29 E	1
Mexico	Teoloyucan	TEO	19.747 N	99.182 W	27.81 N	28.4 W	-6

2 Methodology

2.1 Processing magnetic data

2.2 Isolation of magnetic fluctuations of ionospheric origin

According to [4, 6, 8, 10], we can approach the recordings of a local magnetometer as:

$$H_{loc} = H_{SQ} + H_0 + H_{MT} + H_I, \quad (1)$$

where H_{SQ} is the diurnal variation and H_0 is the monthly baseline. H_{MT} on the other hand are the variations induced due to the magnetospheric currents activity and intensification during GS. Finally, H_I stands for the magnetic variations driven by ionospheric currents activity during a GS.

For mid-low magnetic latitudes, we can approach roughly enough H_{MT} as $H_{MT} \approx SYM - H \cdot \cos(\lambda)$, being λ the geomagnetic latitude of certain observatory. Thus H_I can be approached by:

$$H_I = H_{DDEF} + H_{PPEF} \approx H_{loc} - (H_{SQ} + H_0 + SYM - H \cdot \cos(\lambda)) \quad (2)$$

being H_{DDEF} and H_{PPEF} the magnetic field associated with the disturbed dynamo electric fields and the prompt penetration electric fields respectively.

2.3 Time-Frequency Analysis

In order to isolate H_{DDEF} and H_{PPEF} from each other, we can proceed from the consideration that both ionospheric currents induce quasi periodic fluctuation [1, 7, 11]. Hence we begin with a Fourier Analysis, setting passband filters for fluctuations of periods 24 h to reconstruct H_{DDEF} , meanwhile using highpass filters to reconstruct H_{PPEF} .

However, from [2] it is concluded the need of complement the analysis, performing wavelet techniques [9], as shown in [12] where they performed a crosswavelet transform to H_{SQ} and H_I . Thus, they applied a semblance analysis [3]. The purpose of such process is to compare to time series (H_{SQ} and H_I) which have similar band frequency fluctuations ($f \approx 1.15e - 5Hz$ or $T \approx 24h$) identify which signal is more correlated to H_{DDEF} activity.

For the present paper, we performed a wavelet analysis (W), using the Morlet function as mother wavelet. Hence we computed the wavelet spectrum ($|\psi_0|^2$) in order to observe the power of the signal related to H_I . As second stage of this time-frequency analysis, we computed the cross-wavelet:

$$W_n^{SQ, H_I}(s) = W_n^{HSQ}(s)W_n^{H_I*}(s), \quad (3)$$

being s the scale of the wavelet transform, n the index number of each time series. In the right side of equation 3 $W_n^{HSQ}(s)$ is the wavelet transform applied to the diurnal variation meanwhile $W_n^{H_I*}(s)$ is the conjugate of the wavelet transform applied to H_I . The output of this crosswavelet transform we are interested in, are the resulting amplitude α and the local phase θ . Hence we carry out a semblance analysis described by the following equation:

$$semblance = \cos^n(\theta) \quad (4)$$

being n an odd integer number greater than 1. For this work we decided to set $n = 9$ as tested in [3]. From semblance we can obtain a normalized correlation values ranging between -1 and 1, where values closer to -1 are highly correlated to H_I , meanwhile values closer to 1 are more correlated to H_{SQ} . however, considering that semblance does not give information about the intensity of neither of the implied signals, we can multiply it by the amplitude α and compute H_{DDEF} likewise:

$$H_{DDEF} = \alpha \cdot anticorr(semblance), \quad (5)$$

since we are not interested in those signals correlated to H_{SQ} . Having the wavelet spectrum $|\psi_0(n)|^2$ which give us the power of the signals and $\alpha \cdot anticorr(semblance)$ which highlights the signal related to H_{DDEF} , we can observe not only weather H_{DDEF} variations are present during the event but also, their intensity.

3 Results

3.1 Fourier Analysis

3.2 Wavelet Analysis

4 Discussion

5 conclusions

The Ddyn magnetic fluctuations, H_{DDEF} where present in TEO observatory with more intensity since []

Another observation found is that TEO is the point at which we observe picks of H_{PPEF} significantly higher than H_{DDEF} fluctuations, but is also the point at which H_{PPEF} gets highest values during this study,

On the other hand, in the results obtained through analyzing magnetic data from observatories within sector 3 which corresponds to LZH, BMT, CYG, KNY and KAK we observe very weak and even null H_{DDEF} . This is consistent with [...].

Acknowledgements Suspendisse vel felis. Ut lorem lorem, interdum eu, tincidunt sit amet, laoreet vitae, arcu. Aenean faucibus pede eu ante. Praesent enim elit, rutrum at, molestie non, nonummy vel, nisl. Ut lectus eros, malesuada sit amet, fermentum eu, sodales cursus, magna. Donec eu purus. Quisque vehicula, urna sed ultricies auctor, pede lorem egestas dui, et convallis elit erat sed nulla. Donec luctus. Curabitur et nunc. Aliquam dolor odio, commodo pretium, ultricies non, pharetra in, velit. Integer arcu est, nonummy in, fermentum faucibus, egestas vel, odio.

References

- [1] M. Blanc and A. D. Richmond. The ionospheric disturbance dynamo. *Journal of Geophysical Research*, 85(A4):1669–1686, April 1980. doi:10.1029/JA085iA04p01669.
- [2] C.I. Castellanos-Velazco, P. Corona-Romero, J.A. González-Esparza, M.A. Sergeeva, A.L. Caccavari-Garza, and V.J. Gatica-Acevedo. Low latitude geomagnetic response associated with intense geomagnetic storms: Regional space weather in Mexico. *Journal of Atmospheric and Solar-Terrestrial Physics*, 259:106237, 2024. ISSN 1364-6826. doi:https://doi.org/10.1016/j.jastp.2024.106237. URL https://www.sciencedirect.com/science/article/pii/S1364682624000658.
- [3] G. R. J. Cooper and D. R. Cowan. Comparing time series using wavelet-based semblance analysis. *Computers and Geosciences*, 34(2):95–102, February 2008. doi:10.1016/j.cageo.2007.03.009.
- [4] J. W. Gjerloev. The SuperMAG data processing technique. *Journal of Geophysical Research (Space Physics)*, 117(A9):A09213, September 2012. doi:10.1029/2012JA017683.
- [5] INTERMAGNET. International real-time magnetic observatory network, 2021. URL https://www.intermagnet.org/index-eng.php.
- [6] D.J. Knecht and . Shuman B.M. *HANDBOOK OF GEOPHYSICS AND THE SPACE ENVIRONMENT, chapter 4, THE GEOMAGNETIC FIELD*. ed by A. S. Jursa, Boston: Air Force Geophysics Laboratory, 1985.
- [7] Atsuhiro Nishida. Geomagnetic D_p 2 fluctuations and associated magnetospheric phenomena. *Journal of Geophysical Research*, 73(5):1795–1803, March 1968. doi:10.1029/JA073i005p01795.
- [8] Henry Rishbeth and Owen K. Garriott. *Introduction to ionospheric physics*. 1969.

- [9] Christopher Torrence and Gilbert P. Compo. A practical guide to wavelet analysis. *Bulletin of the American Meteorological Society*, 79(1):61 – 78, 1998. doi:10.1175/1520-0477(1998)079<0061:APGTWA>2.0.CO;2. URL https://journals.ametsoc.org/view/journals/bams/79/1/1520-0477_1998_079_0061_apgtwa_2_0_co_2.xml.
- [10] M. van de Kamp. Harmonic quiet-day curves as magnetometer baselines for ionospheric current analyses. *Geoscientific Instrumentation, Methods and Data Systems*, 2(2):289–304, November 2013. doi:10.5194/gi-2-289-2013.
- [11] W. Younas, C. Amory-Mazaudier, Majid Khan, and R. Fleury. Ionospheric and Magnetic Signatures of a Space Weather Event on 25-29 August 2018: CME and HSSWs. *Journal of Geophysical Research (Space Physics)*, 125(8):e27981, August 2020. doi:10.1029/2020JA027981.
- [12] Waqar Younas, C. Amory-Mazaudier, Majid Khan, and M. Le Huy. Magnetic Signatures of Ionospheric Disturbance Dynamo for CME and HSSWs Generated Storms. *Space Weather*, 19(9):e02825, September 2021. doi:10.1029/2021SW002825.